On the selection of FIR bandpass filters for low frequency EEG synchronization applied to A-phase analysis during sleep

Arce-Guevara V.[1] and Alba A.[1] and Mendez M.O.[1]

[1]Facultad de Ciencias, Universidad Autónoma de San Luis Potosí

Abstract— **One way to estimate the instantaneous amplitude and phase of a real-valued signal consists in passing the signal through a bank of quadrature filters. However, a badly designed filter may introduce distortions in the estimations. The objetive of this work is to compare the output phase and amplitude envelope of three bandpass FIR quadrature filters. On the first stage, this study uses as input a synthetic signal whose phase is known, in order to perform a quantitative assessment of the performance of each filter. The bandwidth of the filters is varied in order to see its effect on the output signal. On the second stage, a study of changes in dynamic brain connectivity was made using electroencephalographic data for healthy patients during sleep. Results suggest that the type of filter and its bandwidth must be chosen carefully in order to avoid distortions that may bias the results of any further analysis.**

Index Terms— **Electroencephalography, CAP, biomedical signal processing, biological information theory.**

I. INTRODUCTION

During the analysis of many electrophysiological signals, it is often required to analyze certain components whose frequencies are relatively low, with respect to the bandwidth of the signal, or its sampling rate. One example, in which we are particularly interested, is the analysis of delta waves in electroencephalographic (EEG) signals. The bandwidth of EEG signals is typically defined between 0.1 Hz and 100 Hz, and these signals are often acquired using sampling rates between 100 Hz and 1000 Hz. However, the delta band ranges from 0.1 to 4 Hz, and some authors may even split this range in low-delta (0.1 to 2 Hz) and high-delta (2 Hz to 4 Hz). Depending on the application, the analysis of delta waves may require a careful filter design. One such application is the analysis of transient events during non-REM sleep denominated A-phases, which play an important role in the sleep process [1]. Depending on their frequency content, A-phases can be classified as types A1, A2 or A3, where A1 phases predominantly contain low-frequency waves.

Since the 1970s, and particularly in recent years, the study of synchronization in EEG signals has attracted more attention and interest from researchers. EEG synchronization can be observed in roughly two spatial scales: first, in a local scale, where the degree of synchronization of neural ensembles underlying a single EEG sensor is related to the amplitude of the oscillations observed at that particular EEG channel [2], [3], and second, in a long-range scale, where distant populations of neurons interact and communicate by means of reciprocal long-distance links, producing dynamic changes in the correlation and/or synchronization of the corresponding EEG channels [4]. Both the local and the long-range synchronization are very dynamic, and contain events that may last from a few milliseconds up to several seconds. These changes can often be observed in specific frequency bands. Therefore, in order to study EEG synchronization, a time-frequency decomposition of the raw EEG signals is often required. One way to achieve this consists in passing the signals through a bank of passband filters tuned at the frequencies of interest. The effect of local synchronization can then be measured in terms of the amplitude or energy of the filtered signals, whereas long-range synchronization is often measured using coherence or phase-synchronization measures. Instantaneous amplitude and phase are well defined if the output of each filter is an analytic signal; that is, a complex signal whose imaginary part is the Hilbert transform of the real part. A filter that takes a real signal as input and outputs an analytic signal is called a quadrature filter [5], and has the property that the frequency response to negative frequencies is zero; for this reason, quadrature filters are typically implemented as FIR filters. Among the most popular choices are Gabor filters, whose frequency response is a Gaussian function centered at the tuning frequency [6]. On the other hand, the notion of the phase of a signal only has a physical meaning for periodic signals, such as a sinusoidal, which may be obtained as the output of a very narrow band-pass filter. However, due to the Gabor-Heisenberg uncertainty principle, it is not possible to have an arbitrarily narrow filter, without sacrificing temporal resolution (and computational resources).

Gabor filters are optimal in terms of the uncertainty principle as they provide the best trade-off between temporal resolution and frequency resolution; however, when the tuning frequency is sufficiently low, they may have a significant response to negative frequencies, which causes them to lose their quadrature property. This, in consequence, produces distortions in the recovered amplitude and phase, which may range from mild to severe. A similar issue may arise with typical ideal FIR filters. In contrast, sinusoidal quadrature filters (SQF) have a frequency defined filter which have asymmetrical frequency response which ensures only positive frequencies will be present in the output [7]. In this study, three quadrature FIR filters are subject to various tests

[1] Facultad de Ciencias, Diagonal Sur S/N, Zona Universitaria, San Luis Potosi, S.L.P., Mexico (e-mail: `varce@fc.uaslp.mx`, `fac@fc.uaslp.mx, mmendez@fc.uaslp.mx`).

TRABAJOS LIBRES

in order to evaluate the accuracy of the recovered amplitude envelope and the recovered phase. The filters under study are: a windowed ideal filter, the Gabor filter, and a filter with a sinusoidal frequency response.

To our knowledge, the work presented in [8] do a theoretical study of quadrature filters but used in 2D signals. This study has a practical perspective and is applied for time series or 1D signals. In [5] Picinbono presents the basis for general quadrature filter selection. Instead of a general aproach, our work is more specific because is directed to physiological signals.

II. MATERIALS AND METHODS

A. Synthetic input signal

For the experiments performed, the input signal contains the sum of three cosine waves at frequencies of 1Hz, 4Hz and 8Hz sampled at 256Hz with normally-distributed white noise with zero mean and unit variance.

B. Filters

Since we are particularly interested in the extraction of low-frequency signals, our tests focus on filters with center frequency or tuning frecuencies at 1Hz. In these experiments, the full bandwidth of all filters was set in the range from 0.1Hz to 4Hz with increments of 0.1Hz.

1) Ideal filter: The ideal band-pass filter was constructed using the standard windowing method. An ideal low-pass filter with cutoff parameter ω_c was shifted to center frequency $\omega_e > 0$ using the shift properties of the Fourier transform.

Filter quadrature is guaranteed only when $\omega_e - \omega_c > 0$. Finally a Blackman window $w(n)$ is used to reduce ripples in the frequency response of the filter. The impulse response of the filter is given by:

$$\mathrm{h}_{\omega_c, \omega_e}(n) = \frac{\sin(\omega_c n)}{\pi n} \mathrm{e}^{j\omega_e n} w(n). \tag{1}$$

2) Gabor filter: The impulse response of a Gabor filter is defined as the product of a complex exponential with a Gaussian window, specifically:

$$\mathrm{g}_{\sigma_\omega, \omega_e}(n) = \frac{\sigma_\omega}{\sqrt{2\pi}} \mathrm{e}^{-\frac{\sigma_\omega^2 n^2}{2}} \mathrm{e}^{j\omega_e n}. \tag{2}$$

Gabor filter parameter σ_ω stand for filter bandwidth and ω_e the tuning frequency.

3) Sinusoidal quadrature filter: These filters are defined in the frequency domain in order to obtain an asymmetrical frequency response which is controlled by the tuning frequency ω_k, the bandwidh h and the asymmetric bandwidth component $h_k = min(h, \omega_k)$. The frequency response is given by:

$$S_{h, \omega_e}(w) = \begin{cases} \frac{1}{2}\left[1 + \cos(\frac{\omega - \omega_k}{h_k}\pi)\right] & \text{if } \omega \in [\omega_k - h_k, \omega_k] \\ \frac{1}{2}\left[1 + \cos(\frac{\omega - \omega_k}{h}\pi)\right] & \text{if } \omega \in [\omega_k, \omega_k + h] \\ 0 & \text{otherwise.} \end{cases} \tag{3}$$

The impulse response of this filter is obtained by inverse Fourier transform.
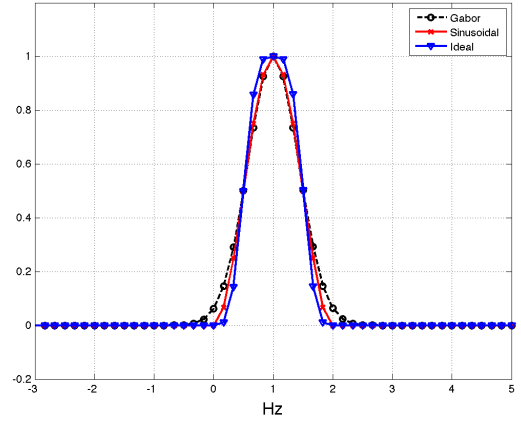
Fig. 1. Frequency response of ideal, Gabor and sinusoidal quadrature filters. All three filter were adjusted with tuning frequency 1Hz and normalized bandwidth of 1Hz.

C. Bandwidth calibration

Because the bandwidth parameter on each filter yields to different effective bandwidth, a bandwidth scaling factor was computed for the Gabor and Ideal filters in order to match their cutoff frequencies to those of the SQF. The cutoff frequencies are defined as those where the power decreases by 3dB. The reduction factor between the Gabor filter bandwidth and sinusoidal filter bandwidth is 2.3529. The scaling factor for ideal filter is 2. The normalized frecuency response magnitude of all filters is shown in Fig. 1.

D. Filter implementation

For each filter tested, the output was calculated by convolution $y_f(n) = h_f(n) * x(n)$ where $y_f(n)$ is the output signal obtained by applying the impulse response of filter $h_f(n)$. Since the filter kernels are complex, a real valued input produces a complex valued output, from which the amplitude envelope and the phase of the output can be measured.

E. Measuring phase distortion

Since the synthetic input signal consist of the sum of three cosine waves, whose frequencies are relatively apart, it is expected that the output of a narrow band-pass filter tuned at one of the input frequencies is a complex exponential, and thus has a linear phase. Distortion takes place when the phase response is not linear in the passband. A measure of the non-linearity of the phase can be obtained using the standard error of the estimate $S_{est} = \sqrt{\sum_{i=1}^{n} \mathrm{e}_i^2 / (n-2)}$, where e_i^2 is the square of the discrepancy between the output phase and the linear model defined by least-square fit.

Another deviation of the filter phase was measured respectly to the true phase. The true phase or expected phase has linear behavior defined by $\theta = 2\pi F_0 / F_s n$ where F_0 is tuning frequency, F_s is the sampling frequency and n is the sample number.

The discrepancy between the true phase and the output phase was measured using $var(d) = \frac{1}{n-1} \sum_{i=1}^{n} (d_i - \bar{d})^2$,
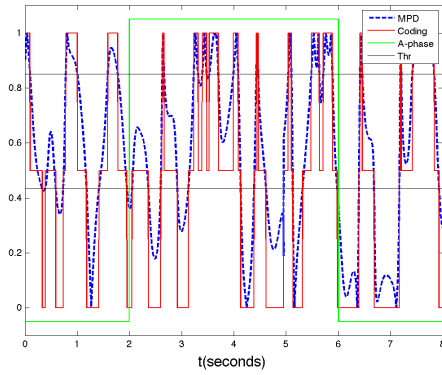
Fig. 2. Discretization of the EEG synchronization in three levels, determined by the quartiles of the baseline distribution, for an A1-phase at sleep stage 3.
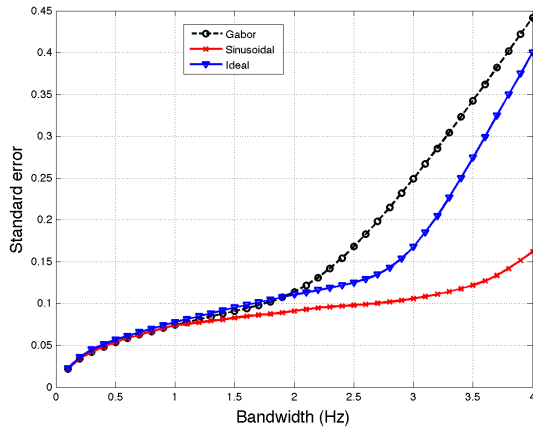
Fig. 3. Non-linearity of the output phase for a noisy input signal.

where d is the diference between the calculated output phase and the true phase θ and n is the number of samples examined.

F. Measuring amplitude envelope variation

Acording to Euler's formula, a pure cosine function can be expresed as $\cos(n) = \frac{1}{2}[e^{j\omega n} + e^{-j\omega n}]$. Exponential term $e^{-j\omega n}$ is named the *negative frequency component* and $e^{j\omega n}$ the *positive frequency component*. Since quadrature filters supress all negative components the magnitude of the output signal is expected to be 0.5. Thus, the error in the amplitude estimation was calculated as $\text{MSE} = \frac{1}{n}\sum_{i=1}^{n}\left(|y_f(i)| - 0.5\right)^2$, Where n is the number of samples of the output (4000 in this study).

G. Synchronization entropy estimation

Entropy is a measure that quantifies the uncertainty of a random variable. In this work, we use Shannon entropy applied to a random variable generated from Electroencephalography (EEG) data.

Polysomnographic data was downloaded from the public Physionet CAP sleep database [9]. The database contains

all night sleep records from 16 healthy patients without any known sleep disease. Records were previously scored by expert neurologists and contains annotations for sleep macrostructure according to Rechtschaffen & Kales rules [10] and CAP annotations as defined by Terzano [1].

Mean Phase Diferrence (MPD) is a way to measure in-phase synchrony. Synchrony between two signals is used to reveal dynamic connectivity patterns. For this analisys, F4C4 and C4A1 EEG channels were selected, but only eight patient records contain both channels, thus our study was limited to those subjects. The phase of the EEG data was obtained by filtering the raw data with quadrature filters tuned to the delta band (0.7-4 Hz). The phase of the resulting analytic signals was used to estimate the normalized measure MPD $\mu(t) = 1 - |wrap(\phi_1(t) - \phi_2(t))|/\pi$, where $\text{wrap}(\phi)$ returns the angle ϕ wrapped to the interval $[-\pi, \pi)$ and ϕ_i represents the phase of channel i.

During most A-phases, the EEG shows a less entropic synchronization pattern; thus our interest lies in evaluating changes in the entropy of EEG synchrony with respect to the baseline segment. The baseline segment is a 2s window prior to the onset of a given A-phase. This baseline is compared with the synchronization observed in a 2s segment right after the onset of a A-phase. Dynamic connectivity was characterized by the entropy of a discretized version of the MPD, which was obtained by classifying every MPD value with respect to the distribution of the MPD during the baseline segment (2s prior to the A-phase onset). MPD values in the first quartile were classified as 0, while values in the last quartile were classified as 1. Any other values were classified as 0.5. Finally, all entropy values are normalized with respect to the entropy of the corresponding baseline segment, which can be shown to be 1.039721. Therefore, the normalized entropy is expected to be less than 1 if the connectivity during the A-phase shows a more organized and stable behavior with respect to the basal state. An example of A1 phase during sleep stage 3 with the corresponding MPD and the discrete version of the MPD can be seen in Fig. 2.

III. RESULTS AND DISCUSSION

A. Quantitative results with a synthetic signal

The RMS deviation of the phase with respect to a straigth line fitted by least-squares regression is shown Fig. 3. When filter bandwidth increases above 1.0Hz, Gabor and ideal filters lose the quadrature property and produce distortions in the output. SQF behaves fairly well until bandwidth exceeds 3Hz. A similar behavior can be observed in Fig. 4 when comparing the recovered phase with the true phase.

The mean square error was used to measure the deviation of the output amplitude envelope from the expected value $0.5|e^{j\omega n}|$. The Fig. 5 shows how the error increases with respect to the bandwidth of the bandpass, especially when negative frequency components are allowed to pass.

B. Entropy of EEG synchronization

The distribution of the normalized entropy for the 2s window into the A1 phases during deep sleep, using the three
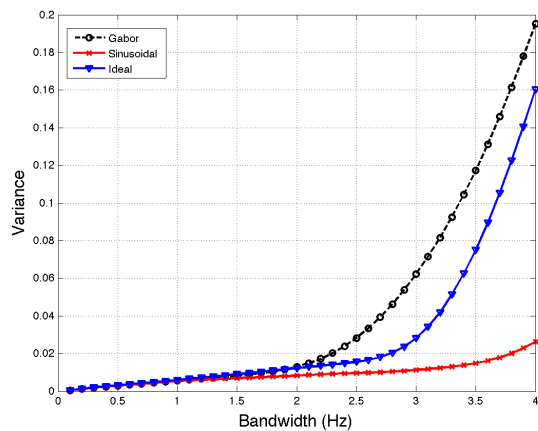
Fig. 4.   Phase estimation error for a noisy input signal.
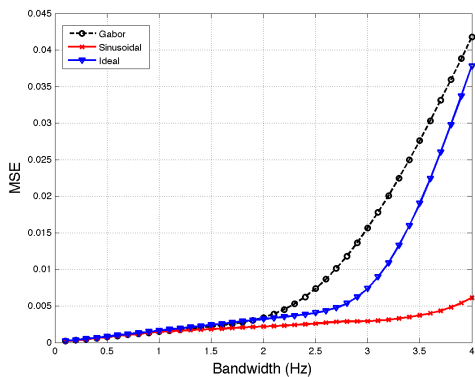
Fig. 5.   Amplitude estimation error for a noisy input signal.

filters under study for EEG synchrony estimation is shown in Fig. 6.

The cutoff frequencies for all filters were set to 0.5Hz and 4Hz (delta band). The sinusoidal and ideal filters maintain a null response to negative frequencies, but the Gabor filter does not. As result the normalized entropies estimated using the Gabor filter are more concentrated around 1, making it more difficult to evaluate changes in the EEG connectivity patterns. A similar behavior is observed for all A-phase subtypes (A1, A2, and A3) by looking at the average normalized entropies, as shown in Table I.

TABLE I
MEAN OF ENTROPY IN SLEEP STAGE 3 & 4

Subtype	Events	Sinusoidal	Ideal	Gabor
A1	1316	0.7959	0.8099	0.8474
A2	190	0.7922	0.8022	0.8466
A3	43	0.8172	0.8290	0.8734

IV. CONCLUSION

This study shows that, from a practical point of view, bandpass filters must be carefully designed when analyzing
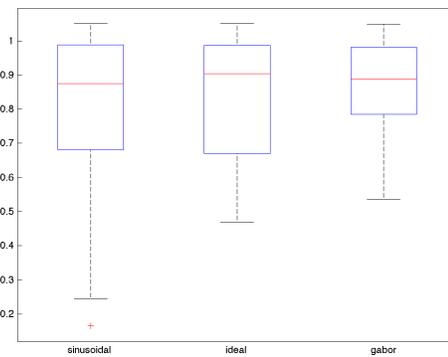
Fig. 6.   Distributions of the normalized entropy for the A1 phases under sleep (sleep stages 3 and 4), estimated using three different quadrature filters.

low-frequency signals. For example, bandwidth parameter must be carefully selected to avoid phase or amplitude distortion. On the other hand, our results show that the sinusoidal quadrature filters maintain the phase stability in presence of noise.

Our interest in activities related to events during the sleep period, led us to determine how significant are the changes in a selected measure. As a measure, we use Shannon entropy to determine the changes of synchrony with respect to the bassline activity. Our results show that a wrong choice of filter (e.g., the Gabor filter in this case) may produce phase artifacts that affect the result of a synchronization analysis at low frequencies.

REFERENCES

[1] M.G. Terzano, L. Parrino, A. Sherieri, R. Chervin, S. Chokroverty, C. Guillem-inault, M. Hirshkowitz, M. Mahowald, H. Moldofsky, A. Rosa, R. Thomas, A. Walters. Atlas, rules, and recording techniques for the scoring of cyclic alternating pattern (CAP) in human sleep. Sleep Med 2001 Nov;2(6):537-553.
[2] G. Pfurtscheller, Graphical display and statistical evaluation of event-related desynchronization (ERD), Electroencephalography and Clinical Neurophysiology, 1977;43:757-60.
[3] G. Pfurtscheller, Event-related synchronization: an electrophysiological correlate of cortical areas at rest, Electroencephalography and Clinical Neurophysiology, 1992;83:62-9.
[4] F.J. Varela, J. P. Lachaux, E. Rodriguez, J. Martinerie, The brainweb: phase synchronization and large–scale integration. Nat Rev Neuroscience, 2001;2: 229-39.
[5] B. Picinbono, On Instantaneous Amplitude and Phase of Signals, IEEE Transactions on Signal Processing, Vol. 45, No. 3, March 1997.
[6] D. Gabor, Theory of communication. Journal of the Institute of Electrical Engineers, 93, 429-457, 1946.
[7] A. Alba, J.L. Marroquin, J. Peña, T. Harmony, B. Gonzalez-Frankenberger. Exploration of event-induced EEG phase synchronization patterns in cognitive tasks using a time– frequency–topography visualization system 2007;161:166–182.
[8] D. Boukerroui, J. A. Noble, M. Brady, On the Choice of Band-Pass Quadrature Filters, Journal of Mathematical Imaging and Vision, July 2004, Volume 21, Issue 1-2, pp 53-80
[9] A. Goldberger, L. Amaral, L. Glass, J. M. Hausdorff, P. Ivanov, R.G. Mark, J. E. Mietus, G. B. Moody, C-K. Peng, H. E. Stanley. PhysioBank, PhysioToolkit, and PhysioNet: Components of a New Research Resource for Complex Physiologic Signals. [Circulation Electronic Pages; http://circ.ahajournals.org/cgi/content/full/101/23/e215]; 2000 (June 13). Circulation 101(23):e215-e220.
[10] A. Rechtscahffen, A. Kales. A manual of standardized terminology, techniques and scoring system for sleep stages in human subjects. National Institutes of Health, Neurological Information Network, Publication 204, 1968.
[11] A.V. Oppenheim, R.W. Schafer, J.R. Buck, Discrete–Time Signal Processing, Prentice Hall Signal Processing Series, 2nd Edition, 1999, ch 7.